Momentum Distribution in a Space Manipulator for Facilitating the Post-Impact Control

Dimitar Nikolaev Dimitrov
Dept. of Aeronautics and Space Engineering
Tohoku University
Aoba01 Sendai 980-8579, Japan
Email: mitko@astro.mech.tohoku.ac.jp

Kazuya Yoshida
Dept. of Aeronautics and Space Engineering
Tohoku University
Aoba01 Sendai 980-8579, Japan
Email: yoshida@astro.mech.tohoku.ac.jp

***Abstract*— This paper presents a new strategy for capturing a free floating satellite initially having angular momentum. The main focus is on the base attitude before, during and after the catch. We use a joint space orthogonal decomposition procedure involving the so-called reaction null space during the pre-impact and post-impact phases. The idea of preloading bias momentum in a space robot system is discussed. Furthermore, we show that if proper post impact control is utilized the base deviation can be minimized.**

I. INTRODUCTION

Capturing a free-floating satellite in space is assumed to be a priority task in recent years. The importance of operations such as re-orbiting a stranded satellite, refueling or assembling components on operational satellites are expected to increase in the near future. Dead satellites in space orbit can jeopardize new missions, therefore their removal is highly recommended. There is one essential problem that has to be dealt with, in order each of these missions to be accomplished, namely capturing operation should be performed.

A capturing operation can be divided into three phases: the pre-impact phase, the impact phase and the post-impact phase. In this paper we are dealing particularly with problems occurring in the first and third one. The main topic presented hereafter is the capture of a free floating satellite initially having angular momentum. The concept of angular momentum distribution over a manipulator chain and practical methods for its management are presented.

Most of the articles addressing the impact phenomenon of free floating manipulator chains analyze the problem from the viewpoint of force impulse generated during the contact. Some useful strategies for determining and minimizing this impulse are developed by Yoshida et al. [1], [2]. By the means of an extended-inverse inertia tensor they developed a comprehensive framework for the impact dynamics. A different strategy regarding the minimization of the impulse throughout a configuration-dependent scalar function is presented in [3]. A comprehensive discussion about the usage of the so-called *reaction null space* is made by Nenchev and Yoshida in [4], [5]. They utilize the null space of the coupling inertia matrix in order to decouple the base and manipulator dynamics. Furthermore they showed that obtaining joint velocities using this approach does not influence the momentum distribution whatsoever. Another

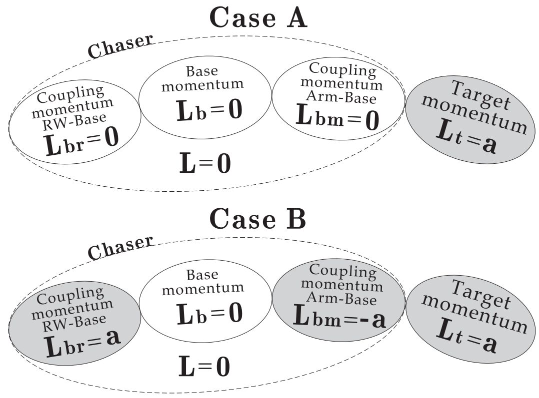

Fig. 1. Two cases of pre-impact angular momentum distribution. $\boldsymbol{L}_{bm}$ and $\boldsymbol{L}_{br}$ are the coupling angular momentums between the base and manipulator, and base and reaction wheels, respectively. $\boldsymbol{L}_b$ denotes the angular momentum stored in the base as a result of its rotational motion, $\boldsymbol{L}$ and $\boldsymbol{L}_t$ are the ones in the chaser and target system, respectively.

approach can be seen in [6], the authors propose a device with controllable momentum wheels ("space leech"), which has to be attached to the target.

Performing a capturing operation in space can lead to different problems. One of them is keeping the base attitude motion within some limits during the approach to the target, the impact and the post-impact motion. In the current paper this is assumed as a priority task, and in order to successfully accomplish it we introduce a new satellite capturing strategy with bias momentum. We should point out that our method is different from the bias method for satellite orientation stabilization using gyrostat (also called *directional stability*).

For a successful completion of a capturing operation, the motion of the entire system after the contact with the target should be considered. Therefore two control laws for angular momentum management during the post-impact phase are proposed as well. Furthermore we emphasize on the fact that the utilization of the bias momentum approach facilitates the control task in the post-impact phase.

The paper is organized as follows. In section II the bias momentum approach is outlined and the relation between angular momentum distribution and base attitude is pointed out. In section III we present preliminaries and main notation. In section IV a useful strategy for angular momentum management is proposed. In section V two control laws for keeping the base attitude deviation zero in the post-impact phase are discussed. The results from a numerical simulation are in section VI. The conclusions are finally given in section VII.

II. The Bias Momentum Approach

One of the main characteristics of a capturing operation in orbit is the momentum conservation if there are no external forces. If just the chaser or target system is considered, it might undergo momentum change, but in the entire system the conservation law will hold. This is valid for the approach, impact and post-impact phases. Recall that our aim is to capture a free floating satellite without changing the chaser's base orientation. In other words, during the three phases of the capturing operation we want the smallest possible amount of angular momentum to be stored in the base rotational motion. This leads to the idea of pre-impact angular momentum distribution. If external forces and torques are not present during the approaching phase, the angular momentum in the entire system consisted of both the chaser and target satellites can be sufficiently defined by four variables (Fig. 1):

(a) $\boldsymbol{L}_{bm}$ - coupling angular momentum between the manipulator and the base.
(b) $\boldsymbol{L}_{br}$ - coupling angular momentum between the reaction wheels and the base.
(c) $\boldsymbol{L}_{b}$ - angular momentum stored in the base as a result of its angular motion.
(d) $\boldsymbol{L}_{t}$ - angular momentum in the target

In Fig. 1 two possible distributions are depicted. In *Case A* just before the contact with the target $\boldsymbol{L}_{bm} = 0$. We call it a non-bias case. After the contact $\boldsymbol{L}_{t}$ distributes over the entire system. How fast it will be transferred to the base depends on factors like: pre-impact configuration, force impulse that occurs during the impact phase, post-impact control. In this paper we assume that no gas-jet thrusters are used on the chaser's base. For attitude stabilization only reaction wheels (RW) are utilized (max. torque of 0.1 Nm; capacity of 16 Nms). As a result of the maximum torque restriction the attitude stabilization devices will not be able to accommodate the angular momentum transferred to the base in a short time. Hence one has to relay on the post-impact control to keep $\boldsymbol{L}_{t}$ in the manipulator and target until it can be accommodated in the reaction wheels. This however is not always conceivable.

One way for facilitating the post-impact control task is reducing the amount of momentum that should be kept in the manipulator and target in the post-impact phase. This can be done if during the approach the momentum distribution depicted in Case B is obtained (*we assume that an approximation of the target's inertia parameters and angular velocity can be done*). Since $\boldsymbol{L}_{bm} = -\boldsymbol{L}_{t}$ with a proper post-impact control law the angular momentum can be redistributed in such a way that the system consisted of base, manipulator and target will come to a complete stop without changing the orientation of the base whatsoever. The distribution in Case B is the most favorable one, since

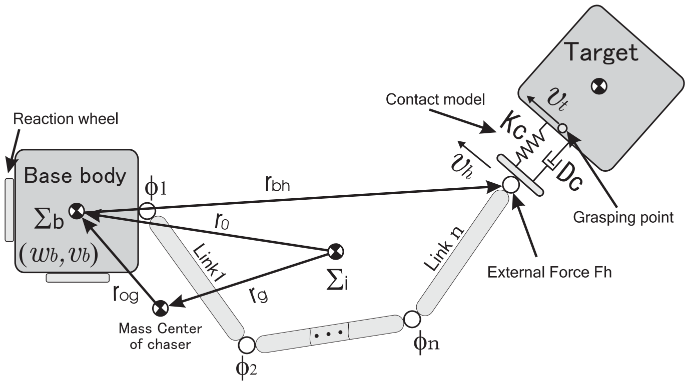

Fig. 2. Model of a n DOF space robot capturing a target

at the start of the post-impact phase the momentum that needs to be managed is actually zero. Hence even servo blocking the joints of the manipulator will stop the motion of the system. However in this case the base might undergo orientation change as a result of the impact force produced at the moment of the contact. A big advantage of the distribution in *Case B* compared to the one in *Case A* is that in the approaching phase there is enough time for obtaining the desired angular momentum distribution. Moreover it can be done without any change in the base attitude.

Obtaining a favorable "full bias" distribution as in Case B is not always possible. The reasons can be lack of additional redundancy in the manipulator arm, or small mass and inertia properties of the links. However, even loading just one part of $\boldsymbol{L}_{t}$ with an opposite sign can improve the performance of the post-impact control. In this paper we call this - partial bias momentum distribution. A contrast between it and a full bias distribution is made in section VI. For a substantial discussion on the bias momentum approach, see [7].

III. Preliminaries and Main Notation

A. Basic equations

The equations governing the motion of a free-flying space robot as a multibody system are in general expressed in the following form:

$$\left[\begin{array}{cc|c} w\boldsymbol{E} & w\hat{\boldsymbol{r}}_{og}{}^T & \boldsymbol{J}_{tg} \\ w\hat{\boldsymbol{r}}_{og} & \boldsymbol{H}_{\omega} & \boldsymbol{H}_{\omega\phi} \\ \hline \boldsymbol{J}_{tg}^T & \boldsymbol{H}_{\omega\phi}^T & \boldsymbol{H}_{\phi} \end{array}\right] \begin{bmatrix} \dot{\boldsymbol{v}}_b \\ \dot{\boldsymbol{\omega}}_b \\ \ddot{\boldsymbol{\phi}} \end{bmatrix} + \begin{bmatrix} \boldsymbol{c}_{b_v} \\ \boldsymbol{c}_{b_\omega} \\ \boldsymbol{c}_{\phi} \end{bmatrix} = \begin{bmatrix} \mathcal{F}_{b_v} \\ \mathcal{F}_{b_\omega} \\ \boldsymbol{\tau} \end{bmatrix} + \begin{bmatrix} \boldsymbol{J}_{b_v}^T \\ \boldsymbol{J}_{b_\omega}^T \\ \boldsymbol{J}_{\phi}^T \end{bmatrix} \mathcal{F}_h \quad (1)$$

where we choose the linear and angular velocity of the base satellite $(\boldsymbol{v}_b, \boldsymbol{\omega}_b)$ and the motion rates of the joints $(\dot{\boldsymbol{\phi}})$ as generalized coordinates. The formulation is not limited to a single manipulator arm, and for the derivations made in this paper we assume a serial manipulator with n Degrees-Of-Freedom (DOF) and a system of reaction wheels, mounted on a base body as shown in Fig. 2. Points of interest are Σ_i and Σ_b, which represent the origin of the inertial frame and the base centroid, respectively. $\boldsymbol{v}_h$ and $\boldsymbol{\omega}_h$ are the linear and angular velocities of the end-effector. Sub-sub-index v or ω stands for the linear or angular part of a six dimensional vector. The symbols used in (1) are defined as follows:

$$\boldsymbol{H}_b = \begin{bmatrix} w\boldsymbol{E} & w\hat{\boldsymbol{r}}_{og}^T \\ w\hat{\boldsymbol{r}}_{og} & \boldsymbol{H}_\omega \end{bmatrix} \in R^{6\times 6}$$

$$\boldsymbol{H}_{ac} = \begin{bmatrix} \boldsymbol{H}_{bm} \; \boldsymbol{H}_{br} \end{bmatrix} = \begin{bmatrix} \boldsymbol{J}_{tg} \\ \boldsymbol{H}_{\omega\phi} \end{bmatrix} \in R^{6\times n}$$

where $\boldsymbol{H}_b(\boldsymbol{x}_b, \boldsymbol{\phi})$ and $\boldsymbol{H}_{ac}(\boldsymbol{x}_b, \boldsymbol{\phi})$ denote the base inertia and the *augmented coupling inertia matrix*, respectively. The latter is consisted of the coupling inertia matrix between the manipulator and the base, and the one between the reaction wheels and the base. $\boldsymbol{x}_b$ stands for the positional and orientational deflection of the base with respect to Σ_i. w is the total mass of the system, $\boldsymbol{E} \in R^{3\times 3}$ is the identity matrix and $\boldsymbol{r}_{og}$ stands for the vector from the total mass center of the system to the centroid of the base (Fig. 2). The $\hat{(\cdot)}$ and $(\cdot)^T$ operators denote a skew-symmetric representation of a three dimensional vector and a matrix transpose, respectively.

$\boldsymbol{c}_b \in R^6$: non-linear term of the base
$\boldsymbol{c}_\phi \in R^6$: non-linear term of the arm and RW
$\boldsymbol{\tau} \in R^n$: torque in the joints.
$\mathcal{F}_h \in R^6$: force and moment exerted on the end-effector.
$\mathcal{F}_b \in R^6$: force and moment exerted on the centroid of the base.

$$\boldsymbol{J}_b^T = \begin{bmatrix} \boldsymbol{J}_{b_v}^T \\ \boldsymbol{J}_{b_w}^T \end{bmatrix} = \begin{bmatrix} \boldsymbol{E} & \boldsymbol{0} \\ \hat{\boldsymbol{r}}_{bh} & \boldsymbol{E} \end{bmatrix} \in R^{6\times 6}$$

where $\boldsymbol{r}_{bh}$ is the distance from the centroid of the base body to the end-effector and $\boldsymbol{0} \in R^{3\times 3}$ is a null matrix. Equation (1) makes use of quantities from the fixed-base manipulators: $\boldsymbol{J}_\phi \in R^{6\times n}$ and $\boldsymbol{H}_\phi \in R^{n\times n}$ denote the Jacobian and the manipulators inertia matrices, respectively. Expressions for the sub-matrices not shown here can be found in [8].

In the next two sub-sections we will briefly overview some useful equations which are to be used as basis for further derivations. The equations in the first sub-section utilize the fact that the satellite-base attitude motion is of greater importance compared to the satellite-base translational motion. In the second one we make some remarks on the so-called reactionless manipulation [9].

B. Angular momentum decomposition

At the moment of the contact, momentum is "exchanged" between the target and the chaser. Especially the angular component of this momentum might be quite harmful. For a satellite-based space robot, it can lead to attitude destabilization. When the robot is mounted on a flexible supporting structure, high amplitude vibrations could be induced. On the other hand the compensation of the linear momentum with the use of external forces is unavoidable, therefore it will not be discussed in this paper. At the beginning of the approaching phase we assume that there is no relative linear velocity between the centroids of the chaser and target satellites. Taking into consideration this, we can reformulate equation (1) with respect to the base attitude only. First eliminate the base acceleration from the upper part of (1) and substitute it in the lower two equations. This will result in equations where $\dot{\boldsymbol{v}}_b$ is implicitly accounted for.

$$\begin{bmatrix} \tilde{\boldsymbol{H}}_b & \tilde{\boldsymbol{H}}_{bm} & \tilde{\boldsymbol{H}}_{br} \\ \tilde{\boldsymbol{H}}_{bm}^T & \tilde{\boldsymbol{H}}_m & \boldsymbol{0} \\ \tilde{\boldsymbol{H}}_{br}^T & \boldsymbol{0} & \tilde{\boldsymbol{H}}_r \end{bmatrix} \begin{bmatrix} \dot{\boldsymbol{\omega}}_b \\ \ddot{\boldsymbol{\phi}}_m \\ \ddot{\boldsymbol{\phi}}_r \end{bmatrix} + \begin{bmatrix} \tilde{\boldsymbol{c}}_b \\ \tilde{\boldsymbol{c}}_m \\ \tilde{\boldsymbol{c}}_r \end{bmatrix} = \begin{bmatrix} \tilde{\mathcal{F}}_b \\ \tilde{\boldsymbol{\tau}}_m \\ \tilde{\boldsymbol{\tau}}_r \end{bmatrix} + \begin{bmatrix} \tilde{\boldsymbol{J}}_b^T \\ \tilde{\boldsymbol{J}}_m^T \\ \tilde{\boldsymbol{J}}_r^T \end{bmatrix} \mathcal{F}_h \quad (2)$$

where sub-indices m and r denote variables of the manipulator and RW, respectively.

Equation (2) provides us with almost all the necessary tools we need in order to control the angular motion of a spacecraft. Integrating the upper part of this set of equations yields the angular momentum conservation law.

$$\boldsymbol{L} = \tilde{\boldsymbol{H}}_b\boldsymbol{\omega}_b + \tilde{\boldsymbol{H}}_{bm}\dot{\boldsymbol{\phi}}_m + \tilde{\boldsymbol{H}}_{br}\dot{\boldsymbol{\phi}}_r + \hat{\boldsymbol{r}}_{og}\boldsymbol{P} + \boldsymbol{r}_0 \times \boldsymbol{P} \quad (3)$$

where $\boldsymbol{P}$ is the linear momentum of the spacecraft, and $\boldsymbol{r}_0$ is the distance from the inertial coordinate frame (Σ_i) to the base centroid (Fig. 2). In equation (3) $\boldsymbol{L}$ is the angular momentum with respect to Σ_i. Utilizing equation (3) one can express the components forming the angular momentum of the chaser satellite during the approaching phase introduced in section II:

$$\boldsymbol{L}_b = \tilde{\boldsymbol{H}}_b\boldsymbol{\omega}_b \;\; ; \;\; \boldsymbol{L}_{bm} = \tilde{\boldsymbol{H}}_{bm}\dot{\boldsymbol{\phi}}_m \;\; ; \;\; \boldsymbol{L}_{br} = \tilde{\boldsymbol{H}}_{br}\dot{\boldsymbol{\phi}}_r$$

If the linear velocity of the centroid of the system is assumed to be zero, and the base does not change its attitude (this can be chosen as a desired condition) one obtains a relation between $\boldsymbol{L}$ and $\dot{\boldsymbol{\phi}}$ by means of the augmented coupling inertia matrix ($\tilde{\boldsymbol{H}}_{ac}$) in which only the base rotation is explicitly accounted for. In the following subsection we will use this relation in order to outline the reaction null space concept.

C. The Null Space Approach

In this section and for the rest of the article we assume that a kinematical redundancy with respect to the base motion task is present. In other words we require the number of manipulator joints (n) to be larger than the number of base variables (m). Recall the note we made on the significance of the base attitude. Now we will formulate the reaction null space with respect to the base attitude only (this technique is also called "selective reaction null space").

Solving equation (3) for the joint velocity rates, assuming $\boldsymbol{\omega}_b = 0$ and $\boldsymbol{P} = 0$, one obtains:

$$\dot{\boldsymbol{\phi}}_m = \tilde{\boldsymbol{H}}_{bm}^+(\boldsymbol{L} - \tilde{\boldsymbol{H}}_{br}\dot{\boldsymbol{\phi}}_r) + \boldsymbol{P}_{RNS}\dot{\boldsymbol{\zeta}} \quad (4)$$

where $\boldsymbol{P}_{RNS} = (\boldsymbol{E}_n - \tilde{\boldsymbol{H}}_{bm}^+\tilde{\boldsymbol{H}}_{bm})$ is the projector onto the null space of $\tilde{\boldsymbol{H}}_{bm}$, $\dot{\boldsymbol{\zeta}} \in R^n$ is an arbitrary vector, $(\cdot)^+$ operator denotes the pseudo inverse of a matrix

(Moore-Penrose generalized inverse) and $\boldsymbol{E}_n \in R^{n\times n}$ is the identity matrix. A well known property of this type of pseudo inverse is the minimization of the norm of $\dot{\boldsymbol{\phi}}_m$ performed in least squares sense. A different type of minimization will be proposed in section V when we will utilize the reaction null space control. $\boldsymbol{P}_{RNS}$ exists if the manipulator is redundant in the sense explained above. For a substantial discussion on the reaction null space approach, see [4], [9].

IV. Angular Momentum Management

The problem of obtaining a desired angular momentum distribution in the chaser system is discussed. Priority task control is introduced.

During the approaching phase the manipulator should follow a desired trajectory in such a way that no base attitude change occurs. Therefore two types of constraints will be imposed: the base attitude and the end-effector motion constraints. If both are of equal importance during the approach to the target, the joint velocities should satisfy both equations (4) and the differential kinematics equation of a free floating space robot (5).

$$\begin{bmatrix} \boldsymbol{v}_h \\ \boldsymbol{\omega}_h \end{bmatrix} = \boldsymbol{J}_m\dot{\boldsymbol{\phi}}_m + \boldsymbol{J}_b \begin{bmatrix} \boldsymbol{v}_b \\ \boldsymbol{\omega}_b \end{bmatrix} \tag{5}$$

This however is not always possible and could lead to unexpected behavior as a result of algorithmic singularities, see [10]. In order to overcome this difficulty one can specify which of the constraints is primary and which secondary. Hence if the control law enters an algorithmic singularity, the secondary constraints will be dropped.

Let us presume that the priority task is keeping the base attitude zero and the secondary one is following a desired trajectory. Substituting $\dot{\boldsymbol{\phi}}_m$ from (4) into (5) we obtain:

$$\begin{bmatrix} \boldsymbol{v}_h \\ \boldsymbol{\omega}_h \end{bmatrix} = \boldsymbol{J}_m^r\dot{\boldsymbol{\zeta}} + \Psi \tag{6}$$

where $\Psi = \boldsymbol{J}_b \begin{bmatrix} \boldsymbol{v}_b^T & \boldsymbol{\omega}_b^T \end{bmatrix} + \boldsymbol{J}_m\tilde{\boldsymbol{H}}_{bm}^+(\boldsymbol{L} - \tilde{\boldsymbol{H}}_{br}\dot{\boldsymbol{\phi}}_r)$ and $\boldsymbol{J}_m^r = \boldsymbol{J}_m\boldsymbol{P}_{RNS}$ is the restricted Jacobian matrix typically appearing in redundancy resolution schemes [11]. Solving (6) for $\dot{\boldsymbol{\zeta}}$ and substituting it back in (4) we obtain:

$$\dot{\boldsymbol{\phi}} = \tilde{\boldsymbol{H}}_{bm}^+(\boldsymbol{L} - \tilde{\boldsymbol{H}}_{br}\dot{\boldsymbol{\phi}}_r) + {\boldsymbol{J}_m^r}^+(\begin{bmatrix} \boldsymbol{v}_h \\ \boldsymbol{\omega}_h \end{bmatrix} - \Psi) \tag{7}$$

In the derivation $\boldsymbol{P}_{RNS}{\boldsymbol{J}_m^r}^+ = {\boldsymbol{J}_m^r}^+$ was used. This relation comes directly from the properties of the pseudo inverse matrix utilized in this paper. Note that even when ${\boldsymbol{J}_m^r}^+$ becomes a null matrix, namely the secondary constraint is dropped, the equation still guarantees reactionless manipulation.

Let us now concentrate on the problem of obtaining a desired angular momentum distribution. Since gas-jet thrusters are not utilized, $\boldsymbol{L}$ will remain constant during the approach to the target. However it will not necessarily be equal to zero. In the general case the system of reaction wheels is used for compensation of environmental torques, therefore before the start of the approach to the target $\tilde{\boldsymbol{H}}_{br}\dot{\boldsymbol{\phi}}_r$ can be different form zero. In the case when $\boldsymbol{L}_{br} \neq 0$ but $\boldsymbol{L}_{bm} = 0$ the angular momentum distribution is still considered as a non-bias one.

Since $\boldsymbol{L}$ is constant during the approach, the only member of equation (7) that can redistribute the momentum in the chaser satellite is $\tilde{\boldsymbol{H}}_{br}\dot{\boldsymbol{\phi}}_r$. On each step it provides information about the angular momentum that is accommodated in the reaction wheels. Since $\boldsymbol{L}_b$ is constrained to be equal to zero, equation (7) will provide such a motion of the manipulator that the rate of change of $\boldsymbol{L}_{bm}$ will be equal to the rate of change of $-\tilde{\boldsymbol{H}}_{br}\dot{\boldsymbol{\phi}}_r$.

V. Post-Impact Phase

After establishing contact with the target, $\boldsymbol{L}_t$ starts distributing over the chaser satellite. Our objective is to manage the angular momentum in such a way that it does not affect the base attitude. Two basic control strategies that would satisfy this desired condition are proposed. In the whole section $\mathcal{F}_h = 0$ and $\mathcal{F}_b = 0$ are assumed.

A. Distributed momentum control (DMC)

The angular momentum conservation equation has a linear form at velocity level. It is much simpler than the equation of motion at acceleration level, and still fully expresses the system dynamics. The knowledge about the angular momentum in the target allows the formulation of a control strategy that utilizes this fact.

So far we used equation (3) only regarding the chaser satellite but in the same manner it could be applied for the target. Only in this case, we assume that a manipulator chain is not available. Therefore the equation becomes:

$$\boldsymbol{L}_t = \tilde{\boldsymbol{H}}_{b_t}\boldsymbol{\omega}_{b_t} + \boldsymbol{r}_{0_t} \times \boldsymbol{P}_t \tag{8}$$

where the sub-script t shows that the variables describe the target satellite. Though having a simple form, the solution of equation (8) in real-time might not be an easy task. The main problem is the on-line measurement of $\boldsymbol{\omega}_{b_t}$. Fortunately its evaluation is not necessary since in the post-impact phase $\boldsymbol{\omega}_{b_t}$ will be equal to $\boldsymbol{\omega}_h$. If however a slip between the gripper and the target occurs, it can be measured through a sensor system positioned on the gripper and the difference between the angular velocities can be considered. The second term ($\boldsymbol{r}_{0_t} \times \boldsymbol{P}_t$) represents the angular momentum of the target as a result of its linear motion. On-line calculation of $\boldsymbol{P}_t$ in the post-impact phase is not necessary. Without loss of generality we can assume that initially $\boldsymbol{P} = \boldsymbol{P}_t = 0$. Hence, though $\boldsymbol{P}$ and $\boldsymbol{P}_t$ will vary during the post-impact phase, they will keep the relation $\boldsymbol{P} = -\boldsymbol{P}_t$.

The knowledge about the angular momentum in the target enables us to combine equations (3) and (8) to obtain $\boldsymbol{L} + \boldsymbol{L}_t = \boldsymbol{L}_{total}$. Solving this equation for the manipulator joint velocities one obtains:

$$\dot{\boldsymbol{\phi}}_m = -\tilde{\boldsymbol{H}}_{bm}^+(\tilde{\boldsymbol{H}}_{b_t}\boldsymbol{\omega}_{b_t} + \tilde{\boldsymbol{H}}_{br}\dot{\boldsymbol{\phi}}_r + f(\boldsymbol{P}) - \boldsymbol{L}_{total}) \tag{9}$$

where $f(\boldsymbol{P}) = \hat{\boldsymbol{r}}_{og}\boldsymbol{P} + \boldsymbol{r}_0 \times \boldsymbol{P} - \boldsymbol{r}_{0_t} \times \boldsymbol{P}$ and $\boldsymbol{\omega}_b = 0$ was assumed. The *distributed momentum control* is simple and with straightforward implementation. It manages the angular momentum in the entire system in such a way that

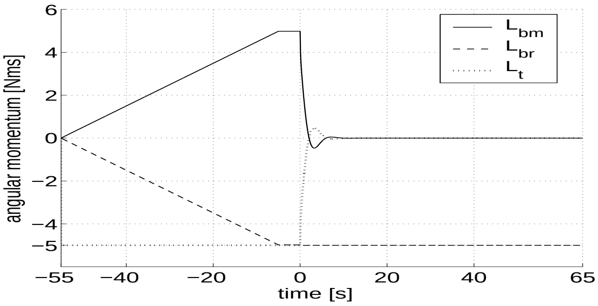

Fig. 3. Angular momentum distribution when full bias momentum is loaded and the joints are blocked after the contact with the target.

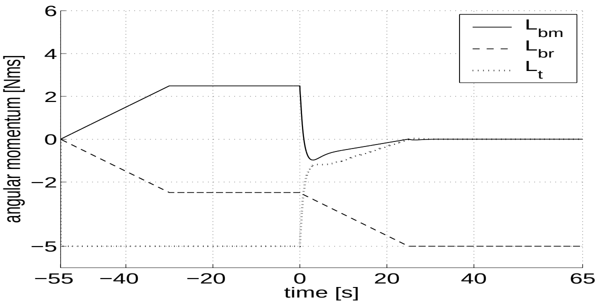

Fig. 4. Angular momentum distribution when partial bias momentum is loaded and DMC is applied.

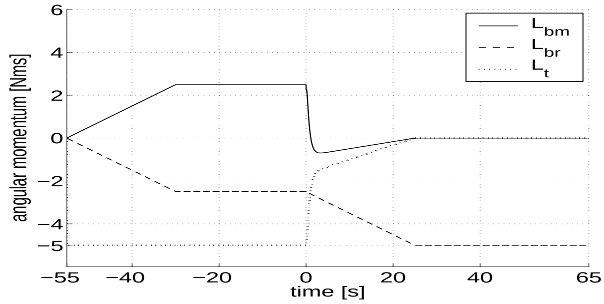

Fig. 5. Angular momentum distribution when partial bias momentum is loaded and RNSC is applied.

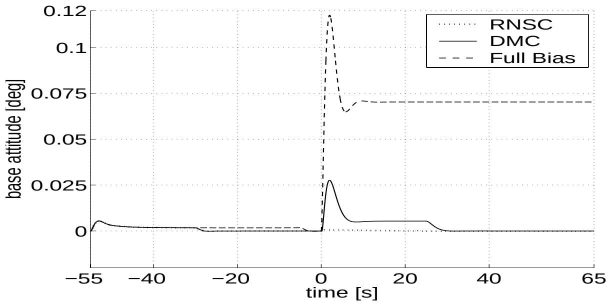

Fig. 6. Base attitude deviation in cases S1, S2 and S3.

no base rotational motion occurs and can be utilized with full as well as with partial bias momentum distribution.

If the measurement of the inertia characteristics and angular velocity of the target is not accurate, $\boldsymbol{L}_{total}$ in equation (9) will be different from the real value. Hence, base rotational motion will occur. Since this can be considered to be the general case, the utilization of a method for on-line parameter identification during the post impact phase is advisable [12].

If a partial bias momentum distribution is obtained during the approaching phase, the reaction wheels should be utilized in order to compensate the remaining angular momentum after the contact with the target. From the viewpoint of (9) this will lead to redistribution of angular momentum between $\tilde{\boldsymbol{H}}_{br}\dot{\boldsymbol{\phi}}_r$ and the remaining members of the equation. Finally when $\tilde{\boldsymbol{H}}_{br}\dot{\boldsymbol{\phi}}_r$ becomes equal to $\boldsymbol{L}_t$ the entire system apart from the reaction wheels will become stationary.

B. Reaction Null Space Control (RNSC)

The transition between the approaching phase and the post-impact phase usually changes the redundancy of the system. In our case there is no need of following a desired trajectory any more, therefore we can utilize the null space of $\tilde{\boldsymbol{H}}_{bm}$ to constrain the system in a different way.

The primary task will be again keeping the base attitude zero and let the secondary one be minimization of the joint velocities. Extracting the first equation from (2) and solving it for $\ddot{\boldsymbol{\phi}}_m$ we obtain:

$$\ddot{\boldsymbol{\phi}}_m = -\tilde{\boldsymbol{H}}_{bm}^{+}(\tilde{\boldsymbol{H}}_b\dot{\boldsymbol{\omega}}_b + \tilde{\boldsymbol{H}}_{br}\ddot{\boldsymbol{\phi}}_r + \tilde{\boldsymbol{c}}_b) + \dot{\boldsymbol{P}}_{RNS}\ddot{\boldsymbol{\zeta}} \qquad (10)$$

where the second term denotes the joint accelerations from the angular reaction null space. Expressing $\ddot{\boldsymbol{\phi}}_r$ from the third equation of (2) and substituting it together with $\ddot{\boldsymbol{\phi}}_m$ from (10) into the middle part of (2) one obtains:

$$\boldsymbol{\tau}_m = \bar{\boldsymbol{H}}\dot{\boldsymbol{\omega}}_b - \bar{\boldsymbol{H}}_r\boldsymbol{\tau}_r + \bar{\boldsymbol{c}} + \tilde{\boldsymbol{H}}_m\dot{\boldsymbol{P}}_{RNS}\ddot{\boldsymbol{\zeta}} \qquad (11)$$

where,

$$\begin{aligned}\bar{\boldsymbol{H}} &= \tilde{\boldsymbol{H}}_{bm}^{T} - \tilde{\boldsymbol{H}}_m\tilde{\boldsymbol{H}}_{bm}^{+}\tilde{\boldsymbol{H}}_b + \bar{\boldsymbol{H}}_r\tilde{\boldsymbol{H}}_{br}^{T}\\ \bar{\boldsymbol{H}}_r &= \tilde{\boldsymbol{H}}_m\tilde{\boldsymbol{H}}_{bm}^{+}\tilde{\boldsymbol{H}}_{br}\tilde{\boldsymbol{H}}_r^{-1}\\ \bar{\boldsymbol{c}} &= \tilde{\boldsymbol{c}}_m - \tilde{\boldsymbol{H}}_m\tilde{\boldsymbol{H}}_{bm}^{+}\tilde{\boldsymbol{c}}_b + \bar{\boldsymbol{H}}_r\tilde{\boldsymbol{c}}_r\end{aligned}$$

With the torque obtained from equation (11) two control tasks could be performed simultaneously.

(a) satellite base attitude control using $\bar{\boldsymbol{H}}\dot{\boldsymbol{\omega}}_b$
(b) manipulator control sub-task using $\tilde{\boldsymbol{H}}_m\dot{\boldsymbol{P}}_{RNS}\ddot{\boldsymbol{\zeta}}$

This control strategy shows that a full decoupling of the base attitude dynamics from the manipulator dynamics can be achieved. Therefore we can use the reaction null space component in order to perform a joint velocity minimization task which will not alter the angular momentum distribution whatsoever. In order to achieve that, one can use a control law similar to the one proposed by Nenchev and Yoshida [4]. Giving the reaction null space and the base attitude components as:

$$\dot{\boldsymbol{P}}_{RNS}\ddot{\boldsymbol{\zeta}} = -\boldsymbol{P}_{RNS}\boldsymbol{K}_m\dot{\boldsymbol{\phi}}_m \quad ; \quad \dot{\boldsymbol{\omega}}_b = -\boldsymbol{K}_b\boldsymbol{\omega}_b$$

where $\boldsymbol{K}_m$ and $\boldsymbol{K}_b$ are gain matrices for manipulator motion and base damping. Substituting them back into (11), the control law becomes:

$$\boldsymbol{\tau}_m = -\bar{\boldsymbol{H}}\boldsymbol{K}_b\boldsymbol{\omega}_b - \bar{\boldsymbol{H}}_r\boldsymbol{\tau}_r + \bar{\boldsymbol{c}} - \tilde{\boldsymbol{H}}_m\boldsymbol{P}_{RNS}\boldsymbol{K}_m\dot{\boldsymbol{\phi}}_m \qquad (12)$$

The first term of (12), guarantees that the manipulator will “absorb” all the angular momentum from the base, and the last one will perform joint velocity minimization.

TABLE I

MODEL PARAMETERS

	base	target	link1	link2	link3	RW
$\boldsymbol{m}$ [kg]	1000	300	100	100	100	10
$\boldsymbol{l}$ [m]	1.0x1.0	1.0x1.0	1.0	1.0	1.0	-
$\boldsymbol{I}$ [kgm^2]	1250	219	33	33	33	0.45

The second component ($\bar{\boldsymbol{H}}_r\boldsymbol{\tau}_r$) accounts for the acceleration change of the RW and is useful when partial bias momentum is utilized during the approaching phase.

In (12) there is no term accounting for the inertia characteristics of the target. Since in the post-impact phase the target will be rigidly fixed to the end effector, one should make a correction of the inertia parameters of the last link in the model. However, even if the exact values of the inertia parameters are not known, equation (12) will still guarantee approximately zero base rotation, provided that the gains are properly chosen. This can be considered as an advantage of the RNSC over the DMC.

VI. SIMULATION STUDY

In this section we present the results from a numerical simulation of a 3 DOF planar manipulator capturing an object loaded with angular momentum. The parameters of the chaser and the target are shown in Table 1.

We assume that prior to the contact the target is rotating with a constant angular velocity of $\boldsymbol{\omega}_t = 0.023$ rad/s. The contact model between the robot hand and the target is approximated with translational and rotational spring-damper system. No gripper is attached to the end point of the manipulator, hence the contact occurs just between two points (at $t = 0$). The inertial frame coincides with the mass center of the entire system.

In this section three cases are discussed, in all of them the end-effector follows the same desired trajectory, the inertia characteristics of the entire system and the initial configuration are identical, at the moment of the contact with the target the linear velocities of the contacting points are nearly the same.

(S1) full bias momentum + blocking the joints (Fig. 3)
(S2) partial bias momentum + DMC (Fig. 4)
(S3) partial bias momentum + RNSC (Fig. 5)

As explained in section IV, in the approaching phase the reaction wheels can be utilized for redistributing the angular momentum in the chaser system. In case S1, during the first 50 sec. of the simulation, -0.1 Nm feed forward torque is applied to the reaction wheel, hence loading a full bias momentum $\boldsymbol{L}_{bm} = 5$ Nms. This distribution remains until $t = 0$. After the contact with the target, the manipulator joints are blocked with a high differential gain. In Fig. 3, almost immediate compensation of $\boldsymbol{L}_t$ with $\boldsymbol{L}_{bm}$ can be observed. The base changes its rotation and settles at a value different from zero (Fig. 6). Because almost no force impulse is generated during the contact with the target the value of this deviation is very small.

In the partial bias momentum case (S2, S3), only half of $\boldsymbol{L}_t$ is preloaded in $\boldsymbol{L}_{bm}$ during the approaching phase. Therefore after the contact with the target and until the reaction wheel successfully loads the remaining half of $\boldsymbol{L}_t$, the manipulator system should "absorb" the angular momentum transferred to the base. The success of this manipulation is not guaranteed because it depends on a variety of conditions like the inertia characteristics of the robot arm, the amount of $\boldsymbol{L}_t$ initially loaded in the target, the joint angle limitations, and others. The bias momentum loaded during the approaching phase will decrease the amount of momentum that should be "absorbed" in the manipulator and therefore facilitates the post-impact control. The angular momentum profile when DMC and RNSC are applied, is depicted in Fig. 4 and 5, respectively. The based attitude motion in both cases is shown in Fig. 6. We want to point out that if one of the two post-impact control laws proposed in this paper is utilized in combination with the full bias momentum, minimal base rotational motion will be guaranteed as well.

VII. CONCLUSIONS

In this paper we discussed the capture of a tumbling satellite by a space robot. The chaser's base attitude motion was assumed to be a priority task. We pointed out that the pre-impact angular momentum distribution is closely related with the attitude profile after the contact with the target. Two post-impact control laws were introduced. Their utilization in combination with the bias momentum approach was outlined.

REFERENCES

[1] K. Yoshida, R. Kurazume, "Modeling of collision dynamics for space free-floating links with extended generalized inertia tensor," *Proc. 1992 IEEE Int. Conf. Robot. Automat.,* Nice, France, pp. 899-904, May 1992.

[2] K. Yoshida, N. Sashida, "Modeling of impact dynamics and impulse minimization for space robots," *Proc. 1993 IEEE/RSJ Int. Conf. Intell. Robots Syst. (IROS'93),* Yokohama, Japan, pp. 2064-2069, July 1993.

[3] L. B. Wee, M. W. Walker, "On the dynamics of contact between space robots and configuration control for impact minimization," *IEEE Trans. Robot. Automat.,* vol. 9, pp. 581-591, Oct. 1999.

[4] D. N. Nenchev, K. Yoshida, "Impact analysis and post-impact motion control issues of a free-floating space robot subject to a force impulse," *IEEE Trans. Robot. Automat.,* vol. 15, no. 3, pp. 548-557, June 1999.

[5] K. Yoshida, D. Nenchev, "Space robot impact analysis and satellite-base impulse minimization using reaction null-space," *Proc. 1995 IEEE Int. Conf. Robot. Automat.,* Nagoya, Aichi, Japan, pp. 1271-1277, May 1995.

[6] M. W. Walker, D. M. Kim, "Satellite stabilization using space leeches," *Proc. IEEE Amer. Contr. Conf.,* San Diego, CA, May 23-25, 1990, pp. 1314-1319.

[7] D. Dimitrov, K. Yoshida, "Utilization of the bias momentum approach for capturing a tumbling satellite," *Proc. IEEE IROS 2004,* Sendai, Japan, (accepted).

[8] K. Yoshida, "Practical coordination control between satellite attitude and manipulator reaction dynamics based on computed momentum concept ," *Proc. 1994 IEEE/RSJ/GI Int. Conf. Intell. Robots Syst. (IROS'94),* Munich, Germany, pp. 1578-1585, Sep. 1994.

[9] K. Yoshida, D. N. Nenchev, "Space robot impact analysis and satellite-base impulse minimization using reaction null space," *Proc. 1995 IEEE Int. Conf. Robot. Automat.,* Nagoya, Japan, pp. 1271-1277, May. 1995.

[10] D. N. Nenchev, Y. Tsumaki, "Singularity-consistent parameterization of robot motion and control," *The Int. J. Robot. Res.,* vol. 19, no. 2, pp. 159-182, Feb. 2000.

[11] D. N. Nenchev, "Restricted Jacobian matrices of redundant manipulators in constrained motion tasks," *Int. J. Robot. Res.,* vol. 11, no. 6, pp. 584-597, 1993.

[12] S. Abiko, K. Yoshida, "On-line parameter identification of JEMRMS based on vibration dynamics for precise end-point control," *24th ISTS,* Miyazaki, Japan, May 30 - June 6, 2004.